7-2 Superconducting Submillimeter-Wave Limb-Emission Sounder on the International Space Station I : Radiometric and Spectral Calibration and Data Processing

OCHIAI Satoshi, NISHIBORI Toshiyuki, OZEKI Hiroyuki, KIKUCHI Ken'ichi, and MANABE Takeshi

Superconducting Submillimeter-wave Limb-Emission Sounder, SMILES, to be aboard the International Space Station has the ability to observe vertical profiles of atmospheric minor constituents by receiving limb-emission spectra from the atmosphere with its high sensitivity and precision at 625- and 650-GHz bands. In this paper, we describe the outline of the calibration algorithm on limb-emission spectra observed by SMILES.

Keywords
SMILES, Atmospheric remote sensing, International Space Station, Sensor calibration, Submillimeter wave

1 Introduction

Superconducting Submillimeter-wave Limb-Emission Sounder (SMILES)[1]-[3] is a sensor for observing the earth's atmosphere and will be aboard the Exposed Facility (EF) of Kibo Japanese Experiment Module (JEM) of the International Space Station. SMILES is scheduled to be launched in the summer of 2009. After SMILES is mounted on the JEM/EF, it will operate in orbit for one year, observing the stratosphere in the latitude range between approximately 65 degrees north and 38 degrees south. SMILES will receive radiation from the direction of the atmospheric limb by scanning the elevation angle, and obtain spectra at a resolution of approximately 1.4 MHz in two frequency bands: from 624.32 GHz to 626.32 GHz and from 649.12 GHz to 650.32 GHz. Through these observations it will be possible to derive the vertical distribution of atmospheric molecules from the stratosphere to the mesosphere, including O_3, HCl, ClO, HOCl, HO_2, HNO_3, CH_3CN, and BrO.

In limb spectral observation, it is essential to obtain highly precise data for the intensity, frequency, and spectral shape of radiation from atmospheric molecules, as well as the position of the field of view. The observed values need to be calibrated to satisfy the specifications required to achieve the goals of the SMILES mission. SMILES is characterized by its pioneering use of a superconducting mixer in space for highly-sensitivity signal detection. The high-sensitivity nature of measurement is expected to reduce random errors in received spectral intensity. Specifically, to maximize the advantage of such small random errors, high precision is required in the absolute value of intensity.

NICT developed a balloon-born limb

sounder using the same frequency as SMILES[4][5] and demonstrated radiometric calibration and retrieval of molecular concentration profiles[6]. The calibration algorithm used in the MLS of the United States' Aura satellite is open to the public[5][6]. The SMILES Mission Team, which consists of members from the Japan Aerospace Exploration Agency (JAXA) and NICT, developed the Data Processing System for Level 0 and 1, and intends to publish a document describing the details of the calibration algorithm used in this system once SMILES begins operation. This article briefly describes the calibration algorithm used in the Data Processing System for SMILES.

2 SMILES calibration process

SMILES data are classified by processing stage: calibrated brightness temperature data (Level 1B), vertical profiles of the minor constituents along the orbit (Level 2), and the higher-order processed data including global mapping (Level 3). The calibration of the observed data with respect to the parameters of the SMILES hardware is related to Level 1 and Level 2 processes. While the Level 2 process analyzes the limb-emission spectra using the highest offset of antenna pointing, beam pattern, and receiver sideband rejection ratio, Level 1 processing involves major calibration of the hardware parameters, and as a result, produces overall calibrated brightness temperature spectra. Here, we briefly describe the calibration algorithm performed in the Level 1B process with respect to the intensity, frequency, and spectral shape of the radiation spectra and the observation position.

2.1 SMILES payload

The SMILES receiver has SIS mixers for two bands: 624.32 GHz to 626.32 GHz and 649.12 GHz to 650.32 GHz. The SSB system noise temperature of the SIS receivers is approximately 500 K. The receivers use a local oscillator at 637.32 GHz, which is common to both bands. The signal received by the antenna is separated into upper sideband (USB) and lower sideband (LSB) by the quasi optics, and each is fed into the corresponding SIS mixer. The antenna is an offset Cassegrain antenna with an elliptical aperture of 400 mm × 200 mm. The antenna scans the beam in the elevation direction in a tangent height range from −35 km to 160 km or larger in the earth's atmosphere and receives atmospheric limb emission and also cosmic background radiation as sources for cold-temperature calibration. The vertical width of the beam at the tangent point is approximately 3.3 km. The system performs further calibration using the calibration hot load within SMILES and the frequency calibration function of the spectrometer. A single observation cycle is designed to be completed in 53 seconds. There are two 1,728-channel Acousto-Optical Spectrometers (AOS) — each with a frequency resolution of 1.4 MHz, frequency channel interval of 0.8 MHz, and bandwidth of 1.2 GHz. These spectrometers allow for the selection of a range to be input into the spectrometer from the receiving band. Figure 1 shows an artist's rendering of the Kibo Japanese Experiment Module (JEM) aboard the International Space Station, where SMILES will be mounted. See references[1]-[3] for further

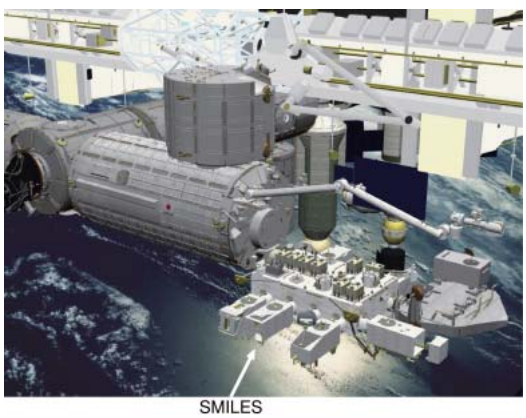

Fig.1 *Artist's rendering of SMILES and Kibo Japanese Experiment Module (JEM) of the International Space Station*

SMILES will be mounted on "Kibo" in the summer of 2009. The figure was provided by JAXA.

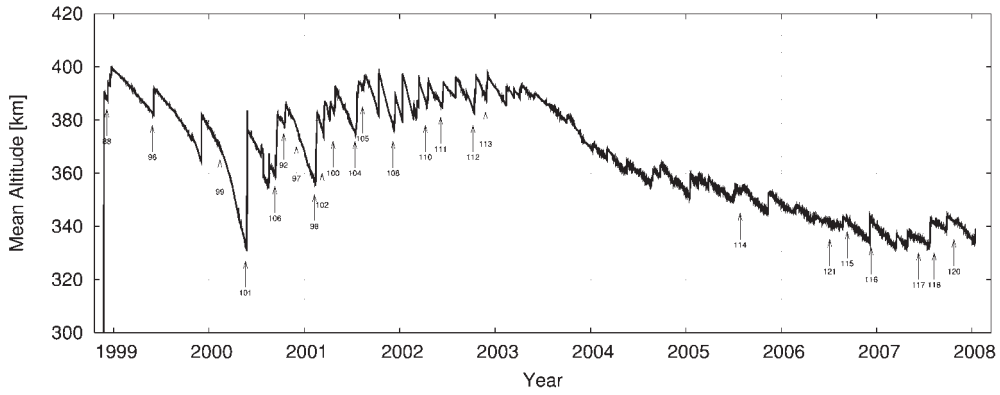

Fig.2 *Mean altitude of ISS*

Mean orbit radius of ISS subtracted from equatorial radius. The arrows in the figure indicate the dates on which the space shuttle will be launched for ISS missions [9].

details of the SMILES payload.

2.2 International Space Station

The International Space Station (ISS) has continued to be built under international collaboration since the launch of the first module in 1998. The ISS is in a nearly circular sun-asynchronous orbit with an inclination of 51.6° at an altitude of approximately 320 km to 420 km from the ground, as shown in Fig. 2. The station performs 15.6 to 15.8 revolutions per day, circling the earth in 91 minutes to 92.5 minutes [9]. The altitude and nominal attitude of ISS vary depending on the configuration during assembly. Although we have not obtained recorded values for fluctuations in attitude, the range allowed in the specifications is within ± 3.5 degrees. The range of latitudes for which SMILES can perform observations is within approximately 0 – 4° north or south from the nominal latitude range, depending on the attitude and altitude of the ISS. Figure 3 shows the range of northest latitudes sampled by SMILES.

2.3 SMILES Data Processing System for Level 0 and Level 1

SMILES mission data is transmitted to the ground via the Medium Rate Data Link (Ethernet) of the ISS. The data can be transmitted through either of the two routes via relay satellites shown in Fig. 4. The SMILES

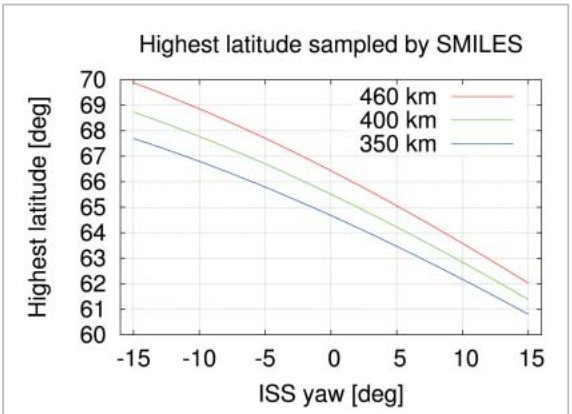

Fig.3 *Northern limit of SMILES observation*

The sampling latitude range of SMILES depends on the attitude and altitude of the ISS. The highest latitude observable is indicated as a function of the attitude.

Experiment Operations System situated in the JAXA facility on the ground receives the telemetry from SMILES and sends commands to SMILES. SMILES is operated by the JAXA facility through these communications. The SMILES Data Processing System analyzes the mission data transmitted from the Medium Rate Data Link, creates Level 0, Level 1A, and Level 1B data, and stores these data (Fig. 4). The facilities within the Experiment Operations System and the lower-level Data Processing System are not connected to the external network on-line. Thus, an operator transfers the data generated in the lower-level Data Processing System off-line to the

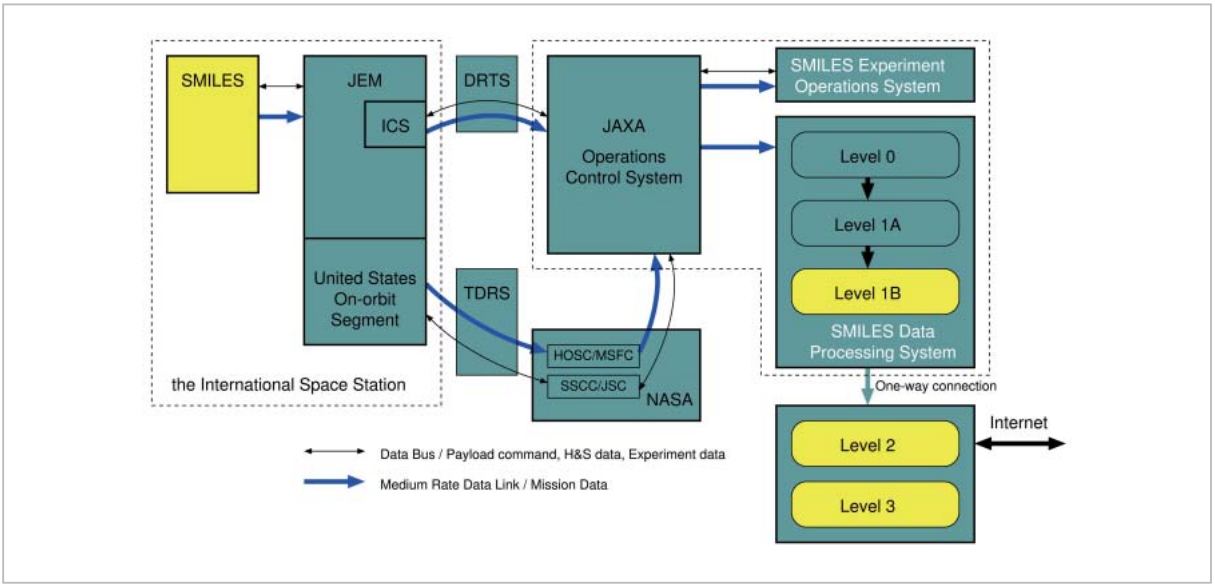

Fig.4 *Observation data flow and SMILES Data Processing System*

Communication with JEM is provided via two routes: via the DRTS data relay satellite of JAXA and via the TDRS satellite of NASA. The mission data is usually downlinked via DRTS.

equipment connected to the external network approximately once each day. Level 2 and subsequent processing is performed in the equipment connected to the external network.

2.4 Interface between SMILES Level 1 process and Level 2 process

Level 1 data comprise the brightness temperature spectrum of the limb emission. A Level 2 process derives the vertical distribution of the molecular concentration based on the brightness temperature spectrum.

An ideal limb-emission brightness temperature spectrum might be obtained by pencil beam observation from a known observation position, does not contain image sidebands, provides sufficiently detailed frequency resolution, and is free from distortion or bias in frequency or intensity. If Level 1 output approaches these conditions, Level 2 and subsequent processing becomes easier. In reality, it is difficult to acquire the ideal limb-emission brightness temperature, so it is practical to use a convoluted spectrum with a smoothing function for Level 1 output and to specify the smoothing function for Level 2 processing. Thus, a spectrum smoothed for observation position and for the frequency axis is passed on to Level 2 and subsequent processing. In this context, we view the offset of antenna pointing and the Doppler-shift offset of frequency as types of smoothing, broadly speaking.

Table 1 summarizes the items processed in the Level 1 process and the smoothing functions passed on as Level 1 output to Level 2 and subsequent processing. Specifically, the smoothing functions employed in Level 2 and subsequent processing consist of the antenna beam pattern, the antenna pointing offset, the frequency response function of the spectrometer, the sideband rejection ratio function, and the Doppler-shift frequency offset. Other items are calibrated in Level 1 processing.

2.5 Brightness temperature calibration

Figure 5 shows a block diagram of the SMILES antenna feed system. The main reflector (MR) of SMILES consists of an offset Cassegrain system with an elliptical aperture of 400 mm × 200 mm. A switching mirror (SWM) placed between the third mirror (RM1) and the fourth mirror (RM 2) periodically introduces a signal from the Calibrated Hot Load (CHL) to enable calibration. The ALP is a part of the SMILES body structure

Table 1 *Interfaces between Level 1 and Level 2*

Items to be corrected	Correction or calulation applied in Level 1 process	Information required for Level 2 process
Antenna beam pattern ($\|Az\|$, $\|El\| \leq 4.2°$ from the beam center)	Spectrum is not corrected	Beam pattern measured on the ground, the inclination angle between elevation axis and the horizon at the tangent point, and the distance between the tangent point and SMILES
Antenna beam pattern ($\|Az\|$, $\|El\| > 4.2°$ from the beam center)	Correction of baseline offset with assumed contribution to the emission from the solid angle beyond ±4.2°	Corrected offset of baseline as reference
Beam loss at main reflector, sub reflector and tertiary mirror	Correctino of loss by reflectors based on the knowledge of ohmic loss of the mirrors and alignment errors	Loss used for correction as reference
Antenna beam pointing	Altitude, latitude, and longitude of the tangent point are calculated from the SMILES attitude and elevation angle	Altitude, latitude, and longitude of the tangent point and the radius of curvature of the Earth
Offset of antenna beam pointing	Correction of beam offset based on the measurements on the ground	Corrected offset as reference
Temperature of the CHL and standing waves of the optics	Brightness temperature of the CHL is calculated based on the temperature sensors on the CHL	Physical temperature of the CHL as reference
Gain fluctuation with long period	Correction of gain fluctuation by interpolating 7 sets of hot and cold calibrations that is acquired every 53 s	Flag indicating that gain fluctuation correction is applied
Relationship between frequencies and channels of the spectrometer	Frequency of each channel is calculated	Frequency of each channel and fitted function of the frequency with 3rd polynomial
Frequency response of the spectrometer	Spectrum is not corrected	Frequency response function measured on the ground
Frequency drift	Spectrum is not corrected	nothing
Sideband response of the receiver	Spectrum is not corrected	Sideband rejection ratio measured on the ground
Doppler shift by the velocity of the ISS	Spectrum is not corrected	Velocity along the line-of-sight at the tangent point
Interference by the sun, the moon, and the sollar paddles	Flagging the case that the main beam or cold sky termination are interfered by the sun, the moon, or the sollar paddle. In case that the main beam directs to the sun, the receiver is protected in advance.	Flags of the interfere by the sun, the moon, and the sollar paddle

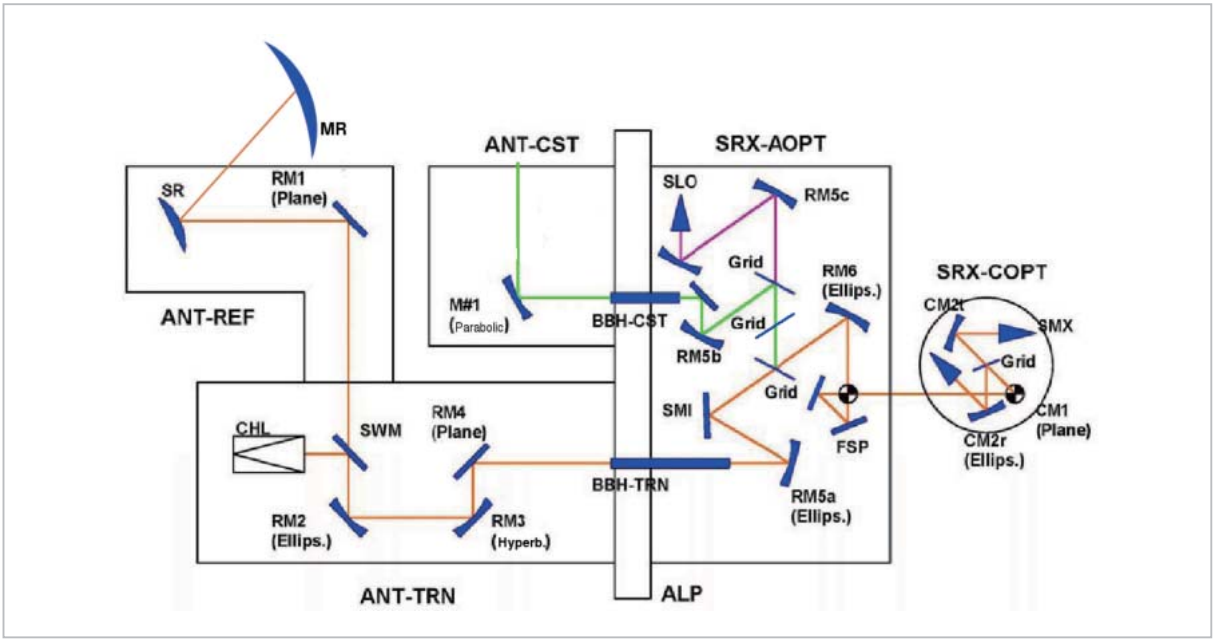

Fig.5 *Block diagram of SMILES antenna feed system*

The limb-emission from the atmosphere is received by the main reflector (MR) with an elliptical aperture of 40 cm × 20 cm, goes through the optics indicated by ANT-REF, ANT-TRN, BBH-TRN, SRX-AOPT, and SRX-COPT, and enters the two superconducting mixers (SMX). See the main text for details. Here ANT-CST contains only a single mirror (M#1) and M#2 in Fig. 2 of reference [3] is therefore incorrect.

and also functions as an electromagnetic shield to protect the devices from the electromagnetic environment of the ISS. The Ambient Temperature Optics (AOPT) also functions as an electromagnetically shielded box further within the structural body. The input port of the AOPT for submillimeter waves is shielded with a back-to-back horn (BBH), essentially

an oversized waveguide, attenuating electromagnetic waves at frequencies of 26.5 GHz or less by 40 dB. In AOPT, SMI converts circularly polarized waves to linearly polarized waves (to reduce the reflections between ANT-TRN and SRX-COPT), and the frequency-selective polarizers (FSPs), which is an interferometric sideband separator specially developed for SMILES application, converts polarizations by 90° in the signal and image bands. COPT uses a wire grid to separate the polarized sidebands and leads the signals into the two superconducting mixers (SMX). Image-band signals added to both mixers are input from ANT-CST. The beam from CST is aimed toward deep space in the direction of the zenith from SMILES. In AOPT, the 637.32-GHz local signal from the submillimeter-wave local oscillator (SLO) is added to a part of the image-band signal from CST.

The brightness temperature of the atmospheric emission is situated between the cosmic background radiation (2.7 K) and the atmospheric temperature (approximately 300 K). Thus, the brightness temperature of the atmospheric emission is determined using radiation of two known temperatures: the radiation from space (2.7 K) and radiation from CHL at approximately 300 K, built-in aboard SMILES. SMILES receives radiation from space, which is used for cold-temperature calibration, by directing the antenna to a tangent height of 160 km or larger. This cold-temperature calibration with the antenna directed upward avoids calibration errors due to loss by mirror reflection, beam leakage, and unnecessary scattering. Nevertheless, we need to be aware that slight effects of the atmosphere still remain. As hot-temperature calibration uses CHL, we need to bear in mind that the beam path of calibration is different from the path provided within the main reflector system. While we use three mirrors when observing the atmosphere (the main reflector, a sub reflector, and a third mirror), we observe CHL by reflection from the switching mirror when performing hot-temperature calibration.

When calibrating the brightness temperature, we need to correct for brightness picked up by the sidelobe of the antenna. Without the appropriate calibration of sources other than the main beam, an antenna with a beam efficiency of 90 % has an error of 10 % or more in received intensity. The width of the beam of the SMILES main reflector is 0.09° in elevation and 0.18° in azimuth. The sidelobe level is −20 dB or less. The beam efficiency is approximately 90 % when defined as 2.5 times the solid angle of the width. The beam pattern from the main reflector is obtained using near-field measurement based on the phase retrieval method, in a manner similar to that used when the beam radiation pattern is obtained for the front side of BBH[10]. The range of the solid angle for which the beam pattern can be obtained by measurement is ± 4.2°, a range that contains approximately 97.5 % of the entire beam. The receiving power entering the antenna from the range of ± 4.2° is expressed as follows in terms of the brightness temperature, denoted as T_{mb}.

$$T_{mb} = \int_{\Omega_{mb}} GT(\theta, \phi) \tag{1}$$

Here, G is the antenna beam pattern measured experimentally on the ground, $T(\theta, \phi)$ is the brightness temperature of the radiation entering from the direction expressed by the elevation angle of θ and the azimuth angle of ϕ, and Ω_{mb} is the range of a solid angle of ± 4.2° from the direction of the beam center of G. Here, we define the brightness temperature, T^*, corresponding to the power of radiation from a black body at a physical temperature of T, received by an antenna with beam efficiency of 1, as follows.

$$T^* = \frac{hf}{k} \frac{1}{\exp\left(\frac{hf}{kT}\right) - 1} \tag{2}$$

Here, f is the frequency, h is Planck's constant, and k is the Boltzmann constant.

The radiation entering the antenna from directions other than Ω_{mb} can be roughly classified into radiation from deep space, radiation from the Earth, and radiation from structural

bodies of SMILES and other structures of the ISS. Denoting the fractions of contributions from these sources as η_{space}, η_{earth}, and η_{body}, respectively, and the respective brightness temperature as T^*_{space}, T^*_{earth}, and T^*_{body}, the total power, T_a, entering the antenna is expressed as follows.

$$T_a = \eta_{mb}T_{mb} + \eta_{space}T^*_{space} + \eta_{earth}T^*_{earth} + \eta_{body}T^*_{body} \quad (3)$$

Here, η_{mb} is the fractional contribution of the beam contained in Ω_{mb}.

As η_{mb} is approximately 0.975, [$\eta_{space} + \eta_{earth} + \eta_{body} \cong 0.025$] holds. Although the contributions from the terms in this expression vary depending on conditions such as the elevation angle of observation and the attitude of SMILES, these values are [$\eta_{earth} \sim 0.0015$] and [$\eta_{body} \sim 0.022$]. The values for η_{earth} and η_{body} can be obtained and corrected by geometrical calculations based on the elevation angle and the attitude. It is safe to assume that the value of T^*_{space} is approximately 0 K at the SMILES observation frequency, although we also use assumed values for T^*_{earth} and T^*_{body}.

Of the entire power, T_a, entering the main reflector, the power T_{RM2} that reaches the fourth mirror (RM2) is expressed as the equation below, given that we need to consider efficiency values, η_{MR}, η_{SR}, and η_{RM1} due to ohmic loss through the main reflector, the sub reflector, and the third mirror (RM1), respectively.

$$T_{RM2} = \eta_{MR}\eta_{SR}\eta_{RM1}T_a + (1 - \eta_{MR}\eta_{SR}\eta_{RM1})T^*_{mirror} \quad (4)$$

Here, we assume the same physical temperature for the main reflector, the sub reflector, and the third mirror, and denote the corresponding brightness temperature as T^*_{mirror}. The values for η_{MR}, η_{SR}, and η_{RM1} should be approximately 0.997. We plan to measure ohmic loss using specimens prepared with the same materials and the same surface treatment as the main and other mirrors of SMILES and to use the measured values accordingly. Losses arise in the main reflector, the sub reflector, and the third mirror other than ohmic loss, such as those due to mirror surface error, mirror edge diffraction, and spillover. Here, we include these losses in the body structure component within the broadband beam pattern of the main reflector.

In cold-temperature calibration, the power T^{cold}_{RM2} that reaches the fourth mirror has the same form as Equations (1) and (4), except that the elevation angle of the main reflector differs.

$$T^{cold}_{RM2} = \eta_{MR}\eta_{SR}\eta_{RM1}T^{cold}_a + (1 - \eta_{MR}\eta_{SR}\eta_{RM1})T^*_{mirror} \quad (5)$$

$$T^{cold}_a = \eta_{mb}T^*_{space} + \eta^{cold}_{space}T^*_{space} + \eta^{cold}_{earth}T^*_{earth} + \eta^{cold}_{body}T^*_{body} \quad (6)$$

Here, we assume that the only radiation that reaches Ω_{mb} is cosmic background radiation. As the antenna elevation angle differs from that in atmospheric limb observation, we assume that η_{space}, η_{earth}, and η_{body} are replaced by η^{cold}_{space}, η^{cold}_{earth}, and η^{cold}_{body}, respectively.

In the calibration by CHL, the power T^{hot}_{RM2} that reaches the fourth mirror is expressed as follows.

$$T^{hot}_{RM2} = \eta_{SWM}T^*_{CHL} + (1 - \eta_{SWM})T^*_{SWM} \quad (7)$$

Here, η_{SWM} is the efficiency of the switching mirror; T^*_{CHL} is the brightness temperature of CHL, and T^*_{SWM} is the equivalent brightness temperature to be added to the switching-mirror loss.

As the reflection from CHL is −60 dB or less[12], when we assume −20-dB reflection on the mixer side, the amplitude of the measured brightness temperature due to the standing wave generated in the optics in CHL measurement is then approximately 3×10^{-6} K. This can be ignored.

We denote the equivalent input system noise temperature of the fourth mirror of the submillimeter-wave receiver as T_{sys}, the total gain of the receiver up to the AOS output as G_{sys}, and the output offset of AOS as V_0. If we assume that these values are unchanged during

calibration, then the AOS output value in atmospheric limb observation (Limb), V_{Limb}; in cold-temperature calibration (Cold), V_{Cold}; and hot-temperature calibration (Hot), V_{Hot}; are expressed as follows.

$$V_{\mathrm{Limb}} = \left\{T_{\mathrm{RM2}} + T_{\mathrm{sys}}\right\} G_{\mathrm{sys}} + V_0 \quad (8)$$

$$V_{\mathrm{Cold}} = \left\{T^{\mathrm{cold}}_{\mathrm{RM2}} + T_{\mathrm{sys}}\right\} G_{\mathrm{sys}} + V_0 \quad (9)$$

$$V_{\mathrm{Hot}} = \left\{T^{\mathrm{hot}}_{\mathrm{RM2}} + T_{\mathrm{sys}}\right\} G_{\mathrm{sys}} + V_0 \quad (10)$$

We define the relative limb spectrum, R_{CAL}, as follows.

$$R_{CAL} = \frac{V_{\mathrm{Limb}} - V_{\mathrm{Cold}}}{V_{\mathrm{Hot}} - V_{\mathrm{Cold}}} \quad (11)$$

Then, from Equations (3) through to (11), we obtain the following expression.

$$\begin{aligned} T_{\mathrm{mb}} = {} & \frac{1}{\eta_{\mathrm{MR}}\eta_{\mathrm{SR}}\eta_{\mathrm{RM1}}\eta_{\mathrm{mb}}} \{\eta_{\mathrm{CHL}}\eta_{\mathrm{SWM}}T^*_{\mathrm{CHL}} + \\ & (1-\eta_{\mathrm{SWM}})T^*_{\mathrm{SWM}} - \eta_{\mathrm{MR}}\eta_{\mathrm{SR}}\eta_{\mathrm{RM1}} \\ & \left(\eta_{\mathrm{mb}}T^*_{\mathrm{space}} + \eta^{\mathrm{cold}}_{\mathrm{space}}T^*_{\mathrm{space}} + \right. \\ & \left. \eta^{\mathrm{cold}}_{\mathrm{earth}}T^*_{\mathrm{earth}} + \eta^{\mathrm{cold}}_{\mathrm{body}}T^*_{\mathrm{body}}\right) - \\ & (1-\eta_{\mathrm{MR}}\eta_{\mathrm{SR}}\eta_{\mathrm{RM1}})\,T^*_{\mathrm{mirror}}\}\ R_{CAL} + \\ & \frac{1}{\eta_{\mathrm{mb}}}\left\{\left(\eta_{\mathrm{mb}} + \eta^{\mathrm{cold}}_{\mathrm{space}} - \eta_{\mathrm{space}}\right)T^*_{\mathrm{space}} + \right. \\ & \left(\eta^{\mathrm{cold}}_{\mathrm{earth}} - \eta_{\mathrm{earth}}\right)T^*_{\mathrm{earth}} + \\ & \left.\left(\eta^{\mathrm{cold}}_{\mathrm{body}} - \eta_{\mathrm{body}}\right)T^*_{\mathrm{body}}\right\} \end{aligned} \quad (12)$$

The Level 1 process obtains the calibrated brightness temperature using Equation (12).

2.6 Sideband ratio

In the SMILES system, FSPs in AOPT separates the sidebands. (See Fig. 5.) The first mixer of SMILES (SMX) is fed the received signal and the 637.32-GHz local signal as input, and outputs an intermediate frequency signal between 11 GHz and 13 GHz. SMX-T (the SMX that receives signals via CM2t) mainly receives LSB signals between 624.32 GHz and 626.32 GHz, and SMX-R (the SMX that receives signals via CM2r) mainly receives USB signals between 649.12 GHz and 650.32 GHz. See reference[11] for the details of the principles of FSP.

We ignore the loss attributable to the optics here and consider the sideband separation characteristics of the optics as set forth below. We express the ratio of the LSB signal transmitted to SMX-R as $R^{\mathrm{LSB}}(f)$ and that transmitted to SMX-T as $[1-R^{\mathrm{LSB}}(f)]$, and the ratio of the USB signal transmitted to SMX-R as $[1-R^{\mathrm{USB}}(f)]$ and that transmitted to SMX-T as $R^{\mathrm{USB}}(f)$. Here, $R^{\mathrm{LSB}}(f)$ and $R^{\mathrm{USB}}(f)$ are functions of the frequency, f.

The sideband ratio depends not only on the characteristics of the optics but also on the characteristics of the mixers. For SMILES, we measured the sideband ratio for the stand-alone AOPT and the sideband characteristics when AOPT and SMX (COPT) are combined. The sideband rejection ratio when AOPT and SMX are combined should differ from the sideband rejection ratio of the stand-alone AOPT only by approximately 1 dB to 2 dB. Thus, here we indicate only the sideband separation characteristics of the stand-alone AOPT. The values $R^{\mathrm{LSB}}(f)$ and $R^{\mathrm{USB}}(f)$ can thus be approximated by the following expressions.

$$R^{\mathrm{LSB}}(f) = m^{\mathrm{LSB}}\left(f - f_0^{\mathrm{LSB}}\right)^2 + a^{\mathrm{LSB}} \quad (13)$$

$$R^{\mathrm{USB}}(f) = m^{\mathrm{USB}}\left(f - f_0^{\mathrm{USB}}\right)^2 + a^{\mathrm{USB}} \quad (14)$$

When the physical temperature of AOPT is t ˚C and its frequency is f GHz, the parameters take the following values.

$$m^{\mathrm{LSB}} = 0.00398 \quad (15)$$

$$f_0^{\mathrm{LSB}} = -2.888012 \times 10^{-4}t^2 + 0.0253396t + 624.75733 \quad (16)$$

$$a^{\mathrm{LSB}} = -2.90103 \times 10^{-7}t + 0.00003150 \quad (17)$$

$$m^{\mathrm{USB}} = 0.00470 \quad (18)$$

$$f_0^{\mathrm{USB}} = 0.0085865t + 648.75572 \quad (19)$$

$$a^{\mathrm{USB}} = -3.30717 \times 10^{-7}t + 0.00006756 \quad (20)$$

The Level 1 process does not correct the sideband characteristics but instead passes the spectrum as is to Level 2 and subsequent processing. Thus, the SMX-R spectrum (Band C)

of the Level 1 output is the sum of the atmospheric spectrum of LSB multiplied by $R^{\mathrm{LSB}}(f)$ and the atmospheric spectrum of USB multiplied by $[1-R^{\mathrm{USB}}(f)]$. Similarly, the SMX-T spectrum (Band A and Band B) is the sum of the atmospheric spectrum of LSB multiplied by $[1-R^{\mathrm{LSB}}(f)]$ and the atmospheric spectrum of USB multiplied by $R^{\mathrm{USB}}(f)$.

2.7 Gain fluctuation correction interpolation

SMILES performs measurements with a period of 53 seconds as a single scan. Each of the generated Level 1 files also contains data for 53 seconds. During the 53-second scan, SMILES use the first 30.5 seconds to observe the limb of the atmosphere from a tangent height of −35 km to approximately 80 km (83 km to 102 km), and then performs cold-temperature calibration at a tangent height of 160 km or larger, frequency calibration of AOS, and hot-temperature calibration with CHL[3].

As there are time differences between limb observation and the cold- and hot-temperature calibrations, gain fluctuation in the receiver causes errors to arise. The main cause of this receiver gain fluctuation is temperature variation. As this temperature variation is slow, it is important to remove any gain fluctuation with periods longer than 53 seconds.

We denote the output data from AOS as $V(i, j, ch)$. Here, i is the scan number (in units of 53 seconds) and j is the data unit number within the scan, which may take a value in the range $[0 \le j \le 105]$, as SMILES acquires a unit of spectral data every 0.5 seconds. The variable ch is the channel number of the spectrometer. There are 1,728 channels, so ch may take a value in the range $[0 \le ch \le 1{,}727]$. We denote the spectrum calculated by subtracting the dark count of AOS, $V^{\mathrm{dark}}(ch)$, from the output as $[A(i, j, ch)\ (= V(i, j, ch) - V^{\mathrm{dark}}(ch))]$. Let us consider obtaining the Hot and Cold spectra at the time of $(i = i_0, j = j_0)$ by interpolating the data. For the scans from $[i_0 - 3]$ to $[i_0 + 3]$, we calculate the average counts, $A_{\mathrm{H}}^{\mathrm{av}}(i, j)$ and $A_{\mathrm{C}}^{\mathrm{av}}(i, j)$, of all channels for the Hot and Cold data units, respectively. In the SMILES scan pattern, the data-unit numbers of the cold-temperature calibration range from 68 to 75, and the data-unit numbers for hot-temperature calibration range from 81 to 88. Thus, we obtain the following equations.

$$A_{\mathrm{H}}^{\mathrm{av}}(i, j) = \frac{\sum_{ch=0}^{1727} A(i, j, ch)}{1728}, j = 81, \cdots, 88 \tag{21}$$

$$A_{\mathrm{C}}^{\mathrm{av}}(i, j) = \frac{\sum_{ch=0}^{1727} A(i, j, ch)}{1728}, j = 68, \cdots, 75 \tag{22}$$

There are 56 values for each of $A_{\mathrm{H}}^{\mathrm{av}}(i, j)$ and $A_{\mathrm{C}}^{\mathrm{av}}(i, j)$. The average count data of the Hot and Cold spectra at the time of $(i = i_0, j = j_0)$, $A_{\mathrm{H}}^{\mathrm{av}}(i_0, j_0)$ and $A_{\mathrm{C}}^{\mathrm{av}}(i_0, j_0)$ are then obtained with the weighted least mean square spline by interpolating the 56 data items. The weighted least mean square spline is the curve determined in this interpolation via the following procedure. The time range of the 56 data items is divided into six intervals (of equal spacing). A cubic function with continuous derivatives up to the second order are prepared for each interval, and the coefficients of the cubic functions are determined to minimize the sum of the square of the difference between the value of the function and the data, with higher weights near the center, under boundary conditions stipulating that the second-order derivatives at both ends are both zero.

The average Hot and Cold spectra, $S_{\mathrm{H}}^{\mathrm{av}}(ch)$ and $S_{\mathrm{C}}^{\mathrm{av}}(ch)$ are calculated using the following equations.

$$S_{\mathrm{H}}^{\mathrm{av}}(ch) = \frac{\sum_{i=-3}^{3}\sum_{j=81}^{88} w_i A(i, j, ch)}{8\sum_{i=-3}^{3} w_i} \tag{23}$$

$$S_{\mathrm{C}}^{\mathrm{av}}(ch) = \frac{\sum_{i=-3}^{3}\sum_{j=68}^{75} w_i A(i, j, ch)}{8\sum_{i=-3}^{3} w_i} \tag{24}$$

Here, w_i is the weight, for example, $\{w_{-3}, w_{-2}, w_{-1}, w_0, w_1, w_2, w_3\} = \{0.1, 0.3, 1.0, 1.0, 0.3, 0.1, 0.0\}$.

With these equations, the Hot and Cold spectra, V_H^{cal} and V_C^{cal} to be used for the data at ($i = i_0$, $j = j_0$) are calculated as follows.

$$V_H^{cal} = \frac{S_H^{av}(ch)A_H^{av}(i_0, j_0)}{\sum_{ch=0}^{1727} S_H^{av}(ch) \Big/ 1728} \quad (25)$$

$$V_C^{cal} = \frac{S_C^{av}(ch)A_C^{av}(i_0, j_0)}{\sum_{ch=0}^{1727} S_C^{av}(ch) \Big/ 1728} \quad (26)$$

2.8 Frequency calibration

In SMILES, the frequencies of the local oscillators can be considered sufficiently stable for both the local oscillator (637.320 GHz) that converts the submillimeter wave signal to the first IF signal and the local oscillators (9.450 GHz and 14.550 GHz) that convert it to the second IF signal. Regarding AOS, a comb signal is input in every scan for calibration. The comb signal has harmonics of 100 MHz, as shown in Fig. 6. As AOS of SMILES covers the approximate range of 1.5 GHz to 2.8 GHz, we can see 14 lines. The frequencies are calibrated based on the position of these lines.

The antenna of SMILES has a line-of-sight vector in the direction 45° diagonally to the left with reference to the direction of velocity of the ISS. The component of the relative velocity of the ISS in the direction of the SMILES line-of-sight is 4.6 km/s to 5.3 km/s. Atmospheric emission undergoes the Doppler shift based on this velocity of 4.6 km/s to 5.3 km/s, which causes a frequency shift of approximately 10 MHz to 11.4 MHz for a signal of 649 GHz. The magnitude of the Doppler shift is a function of several parameters, including the altitude of the ISS and the observation latitude. Figure 7 shows the magnitude of the relative velocity of the tangent point and the Doppler shift without wind when

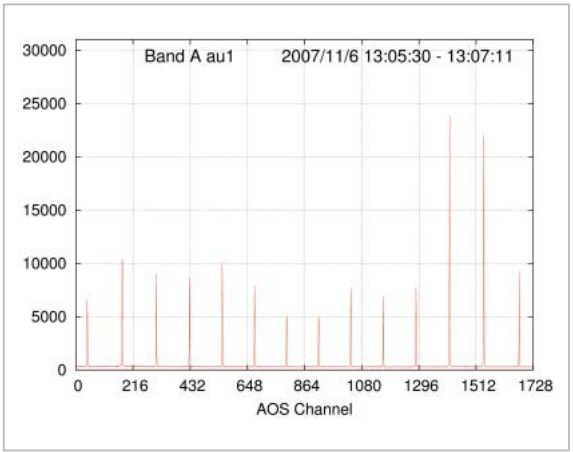

Fig.6 *Example of comb signal input to AOS*

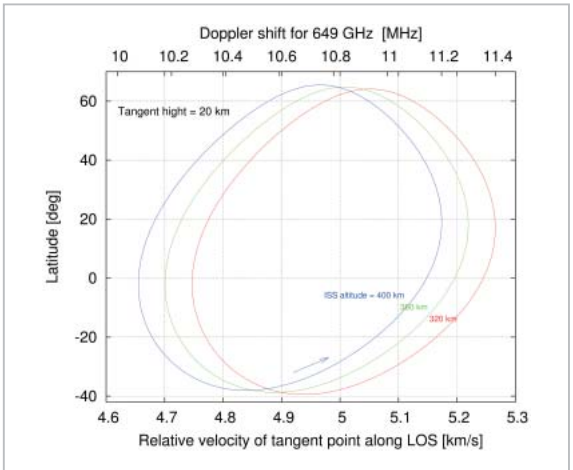

Fig.7 *Estimation of Doppler shift at different latitudes*

The magnitude of Doppler shift (horizontal axis above) versus the latitude (vertical axis) when the wind velocity is zero, the attitude of the ISS is nominal, and the tangent height is 20 km.

the attitude is nominal and the tangent height is 20 km. The Doppler shift is larger when the tangent height is larger, increasing 0.16 MHz to 0.17 MHz per 100 km of height.

In Level 1 output, the spectrum contains the signal of the image band, which undergoes the Doppler shift in the direction opposite the signal band when viewed in the IF frequency. Thus, we decided to perform frequency correction for the Doppler shift in the later stages, instead of at Level 1. Level 1 provides the velocity in the line-of-sight direction of the tangent point.

2.9 Geometrical tangent height

Assuming that the atmosphere consists of thin layers perpendicular to the normal of the surface of an ellipsoidal body, we define the tangent point as the point through which the line-of-sight (LOS) of the limb observation goes through the lowest layer, and the height of the tangent point as the tangent height. In this definition, when a normal at a point on the ground and the LOS are perpendicular to each other, and this normal intersects with the LOS, the intersection is the tangent point. It is difficult to obtain the tangent height analytically when we assume the Earth to have an ellipsoidal body and when we have the LOS in an arbitrary direction. Level 1 processing obtains the point on the ground that satisfies the above conditions by iteration. Here, when the LOS is in the meridian plane, it is also possible to obtain the tangent height using the method described in reference[8]. When the LOS is not in the meridian plane, the method of reference[8] is not correct. With SMILES, the direction of LOS changes in the range between −7° and 100°, so we cannot use the method set forth in reference[8].

The tangent height obtained in Level 1 is the geometrical tangent height. Level 2 and subsequent processing provides the true tangent height with the curvature of the LOS due to the refraction index of the atmosphere taken into consideration.

Level 1 processing provides the geometrical tangent height and also parameters such as the radius of curvature of the Earth, R_c, the distance between the tangent point and SMILES, and the LOS azimuth angle θ_{AZ}. Here, R_c is calculated using the following equations.

$$\frac{1}{R_c} = \frac{\cos^2(\theta_{AZ})}{R_{NS}} + \frac{\sin^2(\theta_{AZ})}{R_{EW}} \quad (27)$$

$$R_{EW} = \frac{R_0}{\left(1 - e^2 \sin^2 \phi\right)^{\frac{1}{2}}} \quad (28)$$

$$R_{NS} = \frac{R_0(1 - e^2)}{\left(1 - e^2 \sin^2 \phi\right)^{\frac{3}{2}}} \quad (29)$$

Here, ϕ is the latitude of the tangent point, R_0 is the equatorial radius (6,378.137 km), and e is the eccentricity of the Earth ellipsoidal ($=\sqrt{[2f - f^2]}$).

2.10 Level 1 data structure

There are three types of SMILES Level 1 data: Level 1A, Level 1B, and Level 1B_REV. Level 1A is files containing the necessary data extracted from the Level 0 data. Level 1B and Level 1B_REV have the same format, but Level 1B_REV is processed with gain fluctuation correction and interpolation, while Level 1B is processed with only the data obtained during a single scan.

A single file of Level 1B data contains data for a single scan of 53 seconds and consists of the following items: status, time, observation position, frequency calibration, brightness temperature, H&K, and ISS supplementary. Among these data, the brightness temperature data in particular are composed of the brightness temperature (calibrated as described in the previous section); the observation-position data are composed of information required in Level 2 and subsequent processing, including the tangent height, the observation latitude and longitude, the distance between the tangent point and SMILES, the radius of curvature of the earth, and the relative velocity along the LOS. The SMILES Mission Team will provide a description of the detailed data format of Level 1B data when this data is published.

3 Conclusions

The algorithm of the SMILES calibration process discussed in this article is implemented in the SMILES Data Processing System for Level 0 and Level 1 developed in 2006. The SMILES hardware is being tested for the launch scheduled in 2009. While the hardware test results are collected, the SMILES Mission Team is determining and improving upon the parameters used in calibration. The SMILES Mission Team will compile the findings obtained in these development activities and

plans to create a set of documents ("algorithm theoretical basis documents," or ATBD) that will describe the details of the algorithm used in SMILES data processing. This article briefly describes a part of the calibration process, the details of which are also to be included in the ATBD.

SMILES is being developed jointly by the Japan Aerospace Exploration Agency (JAXA) and the National Institute of Information and Communications Technology (NICT). We would like to take this opportunity to express our sincere gratitude to Dr. Junji Inatani of the National Astronomical Observatory of Japan, who provided us with particularly helpful discussions and collaboration.

References

1 SMILES Science Team and SMILES Mission Team, "JEM/SMILES Mission Plan, Ver. 2.1", available at http://www2.nict.go.jp/y/y222/SMILES/Mission_Plan/.

2 T. Manabe, "Development of Superconducting Submillimeter-Wave Limb-Emission Sounder (JEM/SMILES) aboard the International Space Station", Journal of CRL, 49(2), 2-1, 2002.

3 S. Ochiai, et al., "Development and Ground Tests of Superconducting Submillimeter-Wave Limb-Emission Sounder (SMILES)", Journal of NICT, 54(1/2), 2-1, 2007.

4 Y. Irimajiri, et al., "BSMILES – a balloon-borne superconducting submillimeter-wave limb-emission sounder for stratospheric measurements", IEEE Geoscience and Remote Sensing Letters, 10.1109/LGRS.2005.856712, 3(1), 88-92, 2006.

5 Y. Irimajiri, et al., "BSMILES – A Balloon-Borne Superconducting Submillimeter-Wave Limb-Emission Sounder", Journal of NICT, 54(1/2), 2-3, 2007.

6 S. Ochiai, et al., "Stratospheric Ozone and ClO Measurement Using Balloon-borne Submillimeter Limb Sounder", IEEE Transactions on Geoscience and Remote Sensing, 10.1109/TGRS.2005.845638, 43(6), 1258-1265, 2005.

7 R. F. Jarnot, et al., "Radiometric and spectral performance and calibration of the GHz bands of EOS MLS", IEEE Transactions on Geoscience and Remote Sensing, 10.1109/TGRS.2005.863714, 44(5), 1131-1143, 2006.

8 R. F. Jarnot, et al., "EOS MLS Level 1 data processing algorithm theoretical basis", JPL, Pasadena, CA, Tech. Rep. JPL D-15210, available at http://mls.jpl.nasa.gov/data/datadocs.php.

9 http://www.celestrak.com/

10 T. Manabe, et al., "Measurement and Evaluation of Submillimeter-Wave Antenna Quasioptical Feed System by a Phase Retrieval Method in the 640-GHz Band", IEICE Transactions on Communications, it in press.

11 T. Manabe, et al., "A new configuration of polarization-rotating dual-beam interferometer for space use", IEEE Transactions on Microwave Theory and Techniques, 51(6), 1696-1704, 2003.

12 T. Nishibori, et al., "Submillimeter performance measurement of Calibrated Hot Load (CHL) for JEM/SMILES", Millimeter and Submillimeter Receiever Workshop, P-05, Osaka Prefecture University, 2008, in Japanese.

OCHIAI Satoshi

Senior Researcher, Environment Sensing and Network Group, Applied Electromagnetic Research Center

Microwave Remote Sensing

***NISHIBORI Toshiyuki**, Dr. Eng.*

ISS Science Project Office, Japan Aero-Space Exploration Agency

***OZEKI Hiroyuki**, Dr. Sci.*

Faculty of Science, Toho-University

***KIKUCHI Ken'ichi**, Dr. Sci.*

Nanoelectronics Research Institute, Advanced Industrial Science and Technology

***MANABE Takeshi**, Dr. Eng.*

Osaka Prefecture University